Biol Trace Elem Res
DOI 10.1007/s12011-014-0039-z

Cu^{2+} Inhibits Photosystem II Activities but Enhances Photosystem I Quantum Yield of *Microcystis aeruginosa*

Chunnuan Deng · Xiangliang Pan · Shuzhi Wang · Daoyong Zhang

Received: 26 April 2014 / Accepted: 3 June 2014

Abstract Responses of photosystem I and II activities of *Microcystis aeruginosa* to various concentrations of Cu^{2+} were simultaneously examined using a Dual-PAM-100 fluorometer. Cell growth and contents of chlorophyll *a* were significantly inhibited by Cu^{2+}. Photosystem II activity [*Y*(II)] and electron transport [$rETR_{max}$(II)] were significantly altered by Cu^{2+}. The quantum yield of photosystem II [*Y*(II)] decreased by 29 % at 100 μg L^{-1} Cu^{2+} compared to control. On the contrary, photosystem I was stable under Cu^{2+} stress and showed an obvious increase of quantum yield [*Y*(I)] and electron transport [$rETR_{max}$(I)] due to activation of cyclic electron flow (CEF). Yield of cyclic electron flow [*Y*(CEF)] was enhanced by 17 % at 100 μg L^{-1} Cu^{2+} compared to control. The contribution of linear electron flow to photosystem I [*Y*(II)/*Y*(I)] decreased with increasing Cu^{2+} concentration. Yield of cyclic electron flow [*Y*(CEF)] was negatively correlated with the maximal photosystem II photochemical efficiency (F_v/F_m). In summary, photosystem II was the major target sites of toxicity of Cu^{2+}, while photosystem I activity was enhanced under Cu^{2+} stress.

Keywords Copper · Cyclic electron flow · Dual-PAM-100 · Electron transport · Photosystem I

Introduction

Copper at low concentration is essential for many metabolic processes in plants and microorganisms. Cu^{2+} is an essential element but high levels of Cu^{2+} have toxic effects on organisms. Cu^{2+} is a strong inhibitor of photosynthesis in phytoplankton [1] and thus it has been frequently used as an algaecide [2]. Cu^{2+} (10 μg L^{-1}) substantially reduced algal biomass and chlorophyll content [3]. Exposure to elevated concentrations of Cu^{2+} can increase content of reactive oxygen species [4–6] and the non-selective conductivity of cell membrane and permeability of the plasmalemma [7]. Extensive studies showed that photosystem II (PSII) is very sensitive to Cu^{2+} toxicity [8]. Cu^{2+} influences the reaction centers of PSII and decomposed the light-harvesting pigment chlorophyll *a* [9]. The oxidizing side [10] and water-splitting complex of PSII [11] can be inhibited by Cu^{2+}. Cu^{2+} can inhibit PSII photochemical activity and damage the structure and composition of the thylakoid membrane. Both acceptor and donor sides can become inhibitory sites of copper [12]. Numerous studies show that there are is multiple Cu^{2+}-inhibitory sites associated with PSII-mediated electron transport [12].

Photosystem I (PSI) was found to be less sensitive than PSII under various environmental stresses, including Cu^{2+} stress [13–16]. It is commonly held that electron transport of PSI of plant is less sensitive to toxicity of Cu^{2+} than that of PSII. For example, Ouzounidou [17] found that Cu^{2+}-stressed *Thlaspi* leaves maintained an increased capacity for PSI-driven electron flow. However, the available information of

C. Deng
Key Lab of Plateau Lake Ecology and Global Change, College of Tourism and Geographic Science, Yunnan Normal University, Kunming 650500, China

C. Deng · X. Pan (✉) · S. Wang
Laboratory of Environmental Pollution and Bioremediation, Xinjiang Institute of Ecology and Geography, Chinese Academy of Sciences, Urumqi 830011, China
e-mail: xlpan@ms.xjb.ac.cn

S. Wang
University of Chinese Academy of Sciences, Beijing 100049, China

D. Zhang
State Key Laboratory of Environmental Geochemistry, Institute of Geochemistry, Chinese Academy of Sciences, Guiyang 550002, China

Published online: 13 June 2014

action mode of Cu^{2+} to PSI is still very limited, and further study is important for understanding effects of Cu^{2+} on the whole electron transport chain from PSII to PSI.

Chlorophyll *a* fluorescence technique has been proven to be useful to study effects of environmental stresses on photosynthesis of algae or plant in vivo [13, 18, 19]. The Dual-PAM-100 system (Heinz Walz, Germany) is powerful to simultaneously probe responses and regulation mechanism of PSI and PSII under various stresses [20–22]. In the present study, effects of copper on the activities and electron transport of PSI and PSII in *Microcystis aeruginosa*, one of the most common freshwater cyanobacteria species, were examined. The Dual-PAM-100 chlorophyll fluorometer was used to study the toxic effects of copper on PSI and PSII activities and the regulation mechanism between PSII and PSI in *M. aeruginosa*.

Materials and Methods

Culture of *M. aeruginosa*

M. aeruginosa (FACHB-905) was obtained from the Institute of Hydrobiology, Chinese Academy Sciences. The cyanobacteria cells were cultivated in BG-11 medium [23] at 25 °C and 30 μmol photons m^{-2} s^{-1} illumination with a 12/12-h light/dark cycle. Cyanobacteria cells in the exponential growth phase were transferred into 50 mL conical flasks for copper treatments.

Cu^{2+} Treatment

Copper ($CuSO_4 \cdot 5H_2O$) of analytical grade was dissolved in distilled water. One milliliter of distilled water or various concentrations of Cu^{2+} solution was added into 24 mL of cell suspension to obtain a series of final nominal Cu^{2+} concentrations of 0, 10, 50, 75, and 100 μg L^{-1}. The samples without addition of Cu^{2+} were used as control. The PSI and PSII activities of the cyanobacteria cells after 12 h various treatments were measured. At 24 h, the optical density of cell suspension was recorded at 680 nm. Content of pigments of cells untreated and treated with Cu^{2+} was determined by spectroscopy.

Measurement of Quantum Yield of PSI and PSII

Quantum yield of PSI [Y(I)] and PSII [Y(II)] of *M. aeruginosa* was measured simultaneously with a Dual-PAM-100 system (Heinz Walz, Germany) [24]. All cyanobacteria cell samples were dark-adapted for 15 min prior to measurement. F_0, the minimum fluorescence, was detected by a measuring light at low intensity. A saturating pulse (10,000 μmol photons m^{-2} s^{-1}) was then applied to detect F_m (the maximum fluorescence after dark adaptation). PAM fluorometer only records the part of the fluorescence induced from the probe flash. Therefore, the PAM measures only the changes in the quantum yield of fluorescence and not the absolute change in fluorescence [25]. The maximal change of P700 signal (P_m) was measured through application of a saturation pulse (10,000 μmol photons m^{-2} s^{-1}) after illumination of far-red light for 10 s [26]. A saturating pulse with duration of 300 ms was applied every 20 s after the onset of the actinic light to determine the maximum fluorescence signal (F_m') and maximum $P700^+$ signal (P_m') under the actinic light (27 μmol photons m^{-2} s^{-1}). The slow induction curve was recorded for 120 s to achieve the steady state of the photosynthetic apparatus, and then the actinic light was turned off. The data derived after the final saturating pulse was used for analysis of activities of PSI and PSII based on previously determined F_0, F_m, and P_m [27].

The quantum yields of PSI [Y(I)] and PSII [Y(II)] were measured by saturating pulses during slow induction. Parameters were calculated automatically [26, 28]: $Y(II)=(F_m'-F)/F_m'$, $Y(NO)=F/F_m$, $Y(NPQ)=F/F_m'-F/F_m$ [where Y(II) was the effective photochemical quantum yield of PSII, Y(NO) was the non-regulated energy dissipation, and Y(NPQ) was regulated energy dissipation]; $Y(I)=(P_m'-P)/P_m$, $Y(ND)=(P-P_0)/P_m$, $Y(NA)=(P_m-P_m')/P_m$ [where Y(I) was the effective photochemical quantum yield of PSI, Y(ND) was the quantum yield of non-photochemical energy dissipation in reaction centers due to PSI donor side limitation, and Y(NA) was the quantum yield of non-photochemical energy dissipation of reaction centers due to PSI acceptor side limitation]; $F_v/F_m=(F_m-F_0)/F_m$, the maximal PSII photochemical efficiency.

Calculation of Cyclic Electron Flow and Linear Electron Flow

The quantum yield of cyclic electron flow [Y(CEF)] was the difference between Y(I) and Y(II): $Y(CEF)=Y(I)-Y(II)$ [16, 29]. $Y(CEF)/Y(I)$, $Y(II)/Y(I)$, and $Y(CEF)/Y(II)$ indicated the contribution of cyclic electron flow (CEF) to Y(I), the contribution of linear electron flow (LEF) to Y(I), and the ratio of the quantum yield of CEF to LEF, respectively. The ratio of $Y(II)/Y(I)$ also provided information about the distribution of quantum yield between two photosystems [27–30].

Measurement of Electron Transport of PSI and PSII

Electron transport rates (ETRs) of PSI and PSII, i.e., ETR(I) and ETR(II), were recorded during the measurement of the slow induction curve. Relative electron transport rates, rETR(I) and rETR(II), were calculated automatically [31]. The responses of electron transport in PSI and PSII to increasing PAR from 0 to 849 μmol photons m^{-2} s^{-1} were recorded as the Rapid Light Curves (RLCs). The following parameters

of $rETR_{max}$(I) and $rETR_{max}$(II) in light response reaction were derived from the RLCs according to the exponential function [32]: α, the initial slope of RLC of rETR(I) or rETR(II), which reflected the quantum yield of PSI or PSII [33]; $rETR_{max}$, the maximal electron transport rates in PSI or PSII; I_k, the light saturation of PSI or PSII, was calculated as $rETR_{max}/\alpha$. Photo-inhibition detected by RLCs provides the threshold of irradiance a culture can tolerate and indicates at which light intensities photo damage will occur [27, 34].

Measurement of Cell Growth

After exposure to various concentrations of Cu^{2+} for 24 h, cell growth of the *M. aeruginosa* was measured by recording the optical density at 680 nm (OD_{680}) with a spectrophotometer (UV2800, Unico, Shanghai, China).

Measurement of Content of Pigments

After 24 h exposure to Cu^{2+}, cyanobacteria cells were harvested by centrifugation at 8,000 r min^{-1} at 4 °C for 5 min. The pigments of the cells were extracted with 96 % ethanol for 24 h at 4 °C in the dark followed by centrifugation at 8,000 r min^{-1} and 4 °C for 5 min. Absorption of the supernatant was measured with a spectrophotometer (UV2800, Unico, Shanghai, China). Contents of chlorophyll (Chl) *a* and carotenoids were calculated according to Lichtenthaler and Wellburn [35].

Statistical Analysis

The experiments were done in triplicate for all treatments. Means and standard errors (S.E.) were calculated by the software Origin 6.0. The statistical significance between control and Cu^{2+}-treated samples were subjected to one-way ANOVA (SPSS V16.0) with post hoc Fisher's least significant difference (LSD) test.

Results

Effects of Cu^{2+} on Cell Growth

The *M. aeruginosa* cell growth showed a decreasing trend with increasing Cu^{2+} concentration (Fig. 1). There was significant difference between control and the treatments with various levels of Cu^{2+} (F=7.242, p<0.01). The growth for cells treated with 10 and 100 μg L^{-1} Cu^{2+} was reduced by 10 and 13 % compared to control, respectively. Cell growth was suppressed by 10 μg L^{-1} Cu^{2+}, but did not exhibit further inhibition as Cu^{2+} concentration increased from 10 to 100 μg L^{-1}.

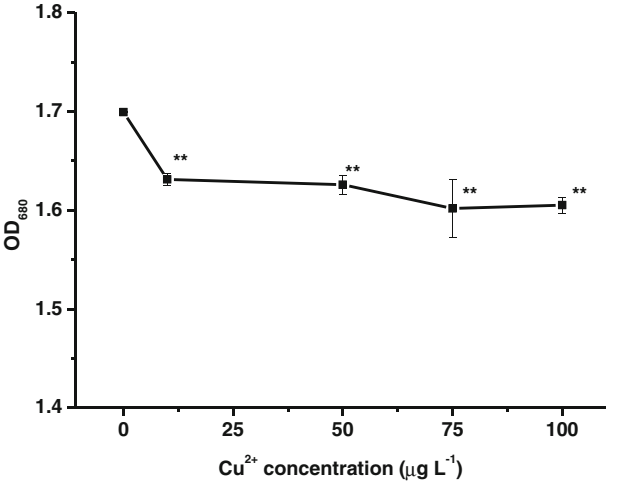

Fig. 1 Growth of *M. aeruginosa* at various Cu^{2+} concentrations expressed as optical density at 680 nm (OD_{680}). Data were means±S.E. (n=3, *p<0.05, **p<0.01)

Effects of Cu^{2+} on Pigments Content

Effects of Cu^{2+} on Chl *a* and carotenoids content in *M. aeruginosa* were shown in Fig. 2. Chl *a* content was affected at high Cu^{2+} concentration (F=4.532, p<0.05). Only 75 and 100 μg L^{-1} Cu^{2+} affected Chl *a* content. For example, Chl *a* content decreased by 23 % at 75 μg L^{-1} Cu^{2+} with respect to control. Carotenoids content of *M. aeruginosa* was not influenced 24 h after exposure to various concentrations of Cu^{2+} (F=0.327, p=0.853).

Effects of Cu^{2+} on Quantum Yield of PSI and PSII

Quantum yield of PSI and PSII were significantly affected after 12 h Cu^{2+} exposure (Table 1). Y(II) (quantum yield of PSII) decreased, associated with an increase of Y(NO) (non-

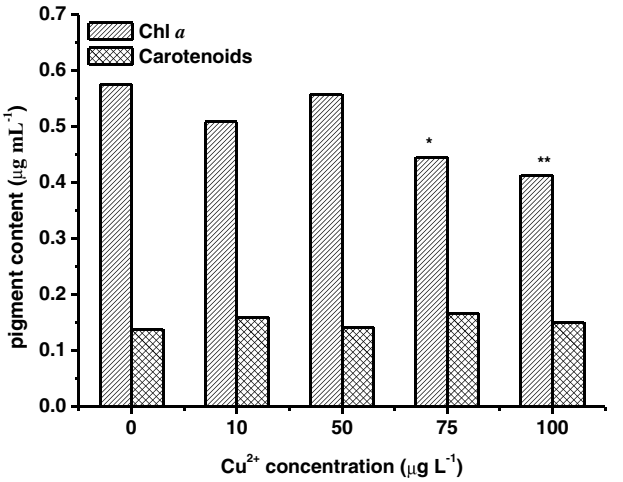

Fig. 2 Concentrations of Chl *a* and carotenoids of *M. aeruginosa* treated with various concentrations of Cu^{2+} for 24 h (n=3, *p<0.05, **p<0.01)

Table 1 Changes of quantum yield of PSI and PSII of *M. aeruginosa* under various concentration of Cu^{2+} after 12 h exposure [*Y*(I), quantum yield of PSI; *Y*(ND), donor side limitation of PSI; *Y*(NA), acceptor side limitation of PSI; *Y*(II), quantum yield of PSII; *Y*(NO), non-regulated energy dissipation. *$p<0.05$ (ANOVA LSD test significance)]

Cu^{2+}(μg L^{-1})	*Y*(I)	*Y*(ND)	*Y*(NA)	*Y*(II)	*Y*(NO)	*Y*(NPQ)
0	0.880±0.032	0.000±0.000	0.120±0.032	0.233±0.002	0.762±0.009	0.006±0.004
10	0.888±0.008	0.000±0.000	0.112±0.008	0.230±0.06	0.752±0.001	0.017±0.007
50	0.913±0.035	0.000±0.000	0.087±0.035	0.192±0.001*	0.785±0.009	0.022±0.009
75	0.917±0.013	0.000±0.000	0.083±0.013	0.141±0.003*	0.846±0.004*	0.013±0.006
100	0.922±0.010	0.000±0.000	0.078±0.010	0.166±0.023*	0.821±0.023*	0.013±0.006

regulated energy dissipation), when Cu^{2+} concentration increased. When Cu^{2+} concentration increased to 100 μg L^{-1}, *Y*(II) decreased by 29 %, while *Y*(NO) increased by 8 % compared to control ($p<0.05$). The maximal PSII photochemical efficiency (F_v/F_m) decreased with the increase of Cu^{2+} concentration (Fig. 3). F_v/F_m for cells treated with 75 and 100 μg L^{-1} Cu^{2+} was only 73 and 75 % of control ($p<0.05$), respectively. Interestingly, *Y*(I) (quantum yield of PSI) increased with increasing Cu^{2+} concentration. *Y*(I) increased by 5 % at 100 μg L^{-1} Cu^{2+} compared to control. *Y*(ND) (PSI donor side limitation) was kept at zero for control and all Cu^{2+} treatments. The value of PSI acceptor side limitation [*Y*(NA)] dropped from 0.12 for control to 0.078 at 100 μg L^{-1} Cu^{2+}.

Effects of Cu^{2+} on Cyclic Electron Flow and Linear Electron Flow

Y(CEF) of *M. aeruginosa* largely increased as Cu^{2+} concentration increased (Fig. 4a). *Y*(CEF) increased by 20 and 17 % at 75 and 100 μg L^{-1} Cu^{2+} with respect to control ($p<0.01$), respectively. *Y*(CEF)/*Y*(I) and *Y*(CEF)/*Y*(II) showed similar change pattern to *Y*(CEF). *Y*(CEF)/*Y*(I) rose from 0.734 for control to 0.821 for 100 μg L^{-1} Cu^{2+}-treated cells ($p<0.01$). *Y*(CEF)/*Y*(II) was enhanced by 71 % and *Y*(II)/*Y*(I) decreased by 33 % at 100 μg L^{-1} Cu^{2+} ($p<0.01$) (Fig. 4b). There is a

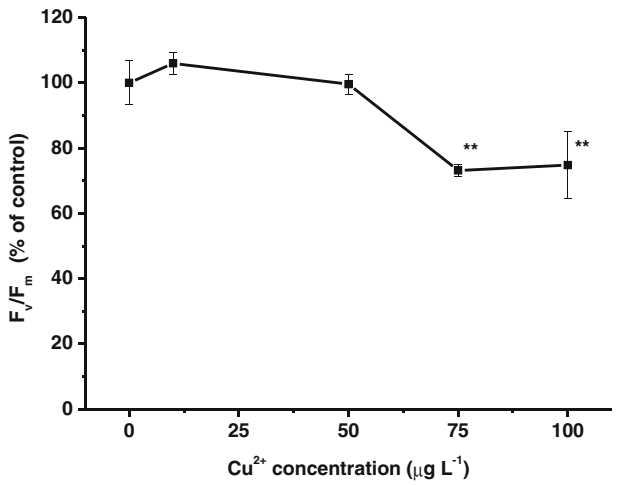

Fig. 3 Effect of Cu^{2+} at various concentrations on maximum efficiency of PSII photochemistry (F_v/F_m) ($n=3$, *$p<0.05$, **$p<0.01$)

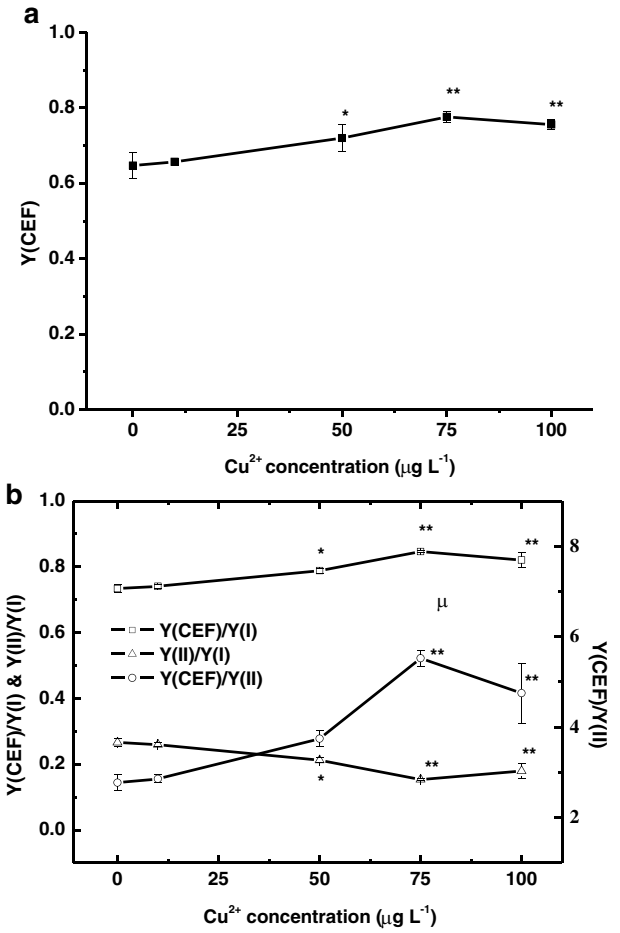

Fig. 4 **a** *Y*(CEF) (the quantum yield of cyclic electron flow) of *M. aeruginosa* exposed to various concentrations of Cu^{2+} for 12 h. Data were derived from the slow induction curves. *Y*(CEF) indicated the difference of quantum yield between PSI and PSII [*Y*(CEF)=*Y*(I)−*Y*(II)] ($n=3$, *$p<0.05$, **$p<0.01$). **b** Ratios of *Y*(CEF)/*Y*(I), *Y*(CEF)/*Y*(II), and *Y*(II)/*Y*(I) of *M. aeruginosa* exposed to various concentrations of Cu^{2+} for 12 h. These ratio were calculated from the value of *Y*(I), *Y*(II), and *Y*(CEF) after exposure to Cu^{2+}. *Y*(CEF)/*Y*(I) means the contribution of cyclic electron flow (CEF) to the yield of PSI. The ratio of *Y*(II)/*Y*(I) indicated that the distribution difference of quantum yield of PSII and PSI, and contribution of linear electron flow (LEF) to PSI. *Y*(CEF)/*Y*(II) means the ration of quantum yield of CEF to that of LEF($n=3$, *$p<0.05$, **$p<0.01$)

significant negative linear correlation between Y(CEF) and F_v/F_m ($p<0.001$) (Fig. 5).

Effects of Cu^{2+} on RLCs of rETR(I) and rETR(II)

To determine the response of the activities of electron transport in PSI and PSII with increasing PAR, rapid light curve was recorded (Fig. 6a, b) and derived parameters from RLCs were calculated (Table 2). The RLCs of rETR(I) at 50 μg L^{-1} Cu^{2+} showed a slight increase while the RLCs of rETR(I) at 100 μg L^{-1} Cu^{2+} declined compared to control. The RLCs of rETR(II) at 10 μg L^{-1} Cu^{2+} declined significantly in the amplitude compared to control. RLCs of rETR(II) showed a significant decrease at higher illuminations while RLCs of rETR(I) increased with increasing light intensity.

In derived parameters from RLCs, $rETR_{max}$(II) significantly decreased with increasing Cu^{2+} concentration (Table 2). $rETR_{max}$(II) at 100 μg L^{-1} Cu^{2+} were only 62 % of control. The values of α(II) decreased significantly and was only 73 % of control for samples treated with 100 μg L^{-1} Cu^{2+}. Compared to control, I_k(II) declined slightly at 50 μg L^{-1} Cu^{2+} but decreased at 100 μg L^{-1} Cu^{2+}. However, electron tranport of PSI showed a different response pattern from that of PSI to Cu^{2+} exposure. $rETR_{max}$(I) increased obviously at 50 μg L^{-1} Cu^{2+} compared to control, but at elevated Cu^{2+} it showed an inhibition too. The values of α(I) presented a upward trend after various Cu^{2+} exposure.

Discussion

In the present study, effects of Cu^{2+} on activities and electron transport of PSI and PSII and the energy regulation mechanism between PSI and PSII in *M. aeruginosa* were analyzed.

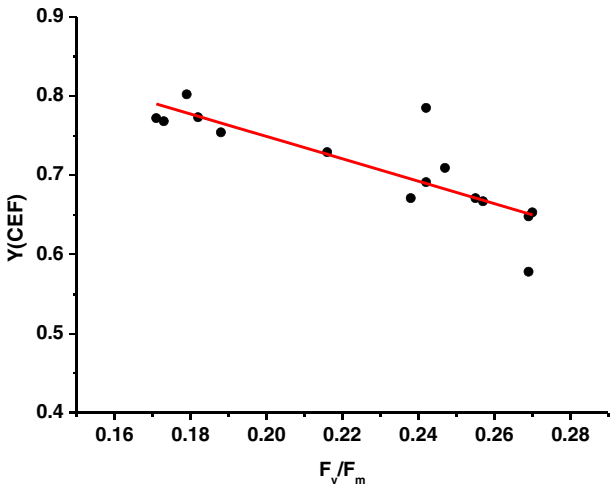

Fig. 5 The relationship between the yield of cyclic electron flow [Y(CEF)] and maximum efficiency of PSII photochemistry (F_v/F_m) (*Correlation coefficients*=−0.837, $p<0.001$)

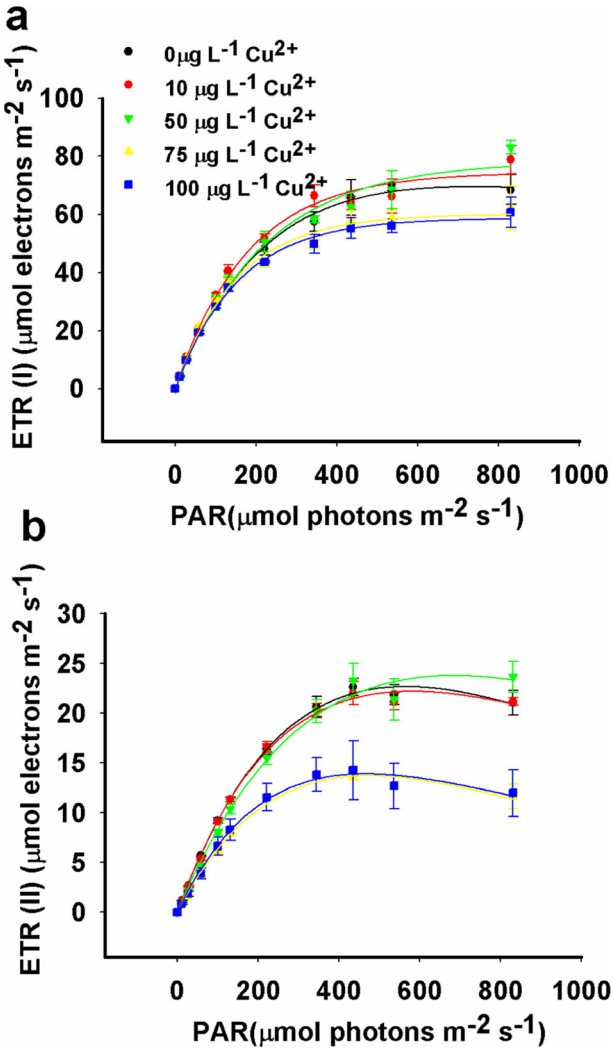

Fig. 6 The rapid light curves (RLCs) of rETR(I) (**a**) and the RLCs of rETR(II) (**b**). Data were detected through the light response reaction after 12 h exposure to 50 and 100 μg L^{-1} Cu^{2+} and control. The RLCs of rETR(I) and rETR(II) were recorded by the Dual-PAM system during the light response reaction, where PAR increased from 0 to 830 μmol photons m^{-2} s^{-1}. All the data presented here were calculated from triplication

It is well established that PSII is sensitive to heavy metal stress [36]. In the present study, the decrease of Y(II) was accompanied with an increase of Y(NO) under Cu^{2+} stress (Table 1). The Y(NO) usually reflects the fraction of energy that is passively dissipated in the form of heat and fluorescence mainly due to the closed PSII centers [24, 37]. It is a good indicator of PSII damage as shown in other studies [27, 37]. The results of the present study suggest that excessive excitation energy cannot be efficiently dissipated into harmless heat [37] and indicate the photodamage of PSII under Cu^{2+} stress. The decrease of Y(II) reflects the inhibitory effect of Cu^{2+} on photochemical energy utilization of PSII, which is further confirmed by the decrease of F_v/F_m. The decrease of F_v/F_m shows the decrease of the fraction of active PSII centers

Table 2 Parameters (α, the initial slope of RLC of ETR; $rETR_{max}$, the maximum electron transport rates; I_k, the light saturation) of electron transport of PSII and PSI derived from the rapid light curves (RLCs) of electron transport rates in PSII [rETR(II)] and electron transport rates in PSI[rETR(I)] under Cu^{2+} stress. Data represent averages of three RLCs means±S.E. (n=3, *p<0.05) (ANOVA LSD test significance)

Cu^{2+}	Parameters of RLCs of rETR(II)			Parameters of RLCs of rETR(I)		
($\mu g\ L^{-1}$)	α(II) (e^- $photon^{-1}$)	$rETR_{max}$(II) ($\mu mol\ e^-\ m^{-2}\ s^{-1}$)	I_k(II) ($\mu mol\ photon\ m^{-2}\ s^{-1}$)	α(I) (e^- $photon^{-1}$)	$rETR_{max}$(I) ($\mu mol\ e^-\ m^{-2}\ s^{-1}$)	I_k(I) ($\mu mol\ photon\ m^{-2}\ s^{-1}$)
0	0.10±0.00	23±1	220±8	0.37±0.02	70±4	189±3
10	0.11±0.01	22±1	214±25	0.48±0.01*	89±12	184±21
50	0.09±0.00	24±2	262±29	0.43±0.02	94±0*	220±8
75	0.07±0.01*	14±0*	212±22	0.46±0.03	72±9	159±26
100	0.07±0.00*	14±2*	191±13	0.43±0.07	66±8	164±32

[38] or the inactivation of the PSII reaction centers. Blockage of electron transport by Cu^{2+} could also lead to a decrease of F_v/F_m [39]. The values of F_v/F_m reflect the potential quantum efficiency of PSII and are usually used as a sensitive indicator of photosynthetic performance of higher plants and algae. However, the F_v/F_m for cyanobacteria is usually underestimated by the influence of cellular phycobiliprotein level and state transitions, but if the carotenoids content is constant, F_v/F_m is still a useful parameter [40, 41]. In the present study, the carotenoids content changed little for each treatment (Fig. 2), which supported that the F_v/F_m values correlated well with changes of PSII function for *M. aeruginosa* (Fig. 5).

Significant inhibition of PSII, cell growth, and Chl *a* synthesis of *M. aeruginosa* was observed under stress of Cu^{2+} (Figs. 1 and 2). The inhibitory effects of Cu^{2+} on photosynthesis are associated with the decrease of Chl *a* content. These results agreed with previous reports [5, 36]. The Cu-induced chlorophyll loss was accompanied by a decreased photosynthetic activity in *Thlaspi* leaves [17]. In the present study, Cu^{2+} exposure lead to a greater decrease of Chl *a* content than the cell growth, which was related to the loss of the capacity for photosynthesis or in the quantum yield of PSII [42]. However, carotenoids content of *M. aeruginosa* was influenced little under Cu^{2+} stress. This was consistent with some previous studies that carotenoid synthesis in stressed conditions was not disturbed and even enhanced to provide photoprotection of cyanobacteria [15]. It is still in controversial that if $CuSO_4$ is an appropriate method for controlling algae. On one hand, some studies showed that addition of copper sulfate to a mature bloom could destroy the cyanobacteria cells but could cause the release of toxins such as microcystin into the water [43]. On the other hand, $CuSO_4$ may decrease the *mcy*D protein transcript abundance, which directly determines the amount of substrate available for microcystin synthesis [6]. Thus, it needs further research to elucidate how $CuSO_4$ influence production of cyanobacterial toxins.

It is commonly held that PSI is less sensitive to copper than PSII [36]. Ouzounidou [17] found that capacity for PSI-driven energy storing electron flow of *Thlaspi* leaves increased under Cu stress. A few studies showed that electron transport in PSI was less sensitive to Cu^{2+} than that in PSII [13, 17]. In the present study, the slightly stimulating effects of Cu^{2+} on photosynthetic quantum yield and electron transport rate of PSI was observed under 10–100 $\mu g\ L^{-1}$ Cu^{2+} stress (Table 1), which was consistent with a few previous studies that PSI was usually more stable than PSII under stresses [16, 44], or PSI activity was even stimulated under heavy metal stress [45]. Other studies showed that PSI was also inhibited by heavy metals. Wodala et al. [46] reported that PSI photochemistry was affected by Cu^{2+} including the decrease of quantum efficiency of PSI, the electron flow in the intersystem chain, and the reduced number of electrons from stromal donors available for PSI. The reported opposite results may be attributed to the differences of the tested materials. In addition, high levles of Cu^{2+} may destroy PSI. The marginal increase of PSI activity in the presence of various concentrations of Cu^{2+} was associated with the decrease of Y(NA) (Table 1). This implies that the increase of quantum yield of PSI was relative to the decrease of limitation of donor side of PSI. This further confirms that PSI is much more tolerant to Cu^{2+} treatment than PSII [17].

The light adaptability and maximal ETR of PSII were obviously inhibited after exposure to Cu^{2+} (Table 2, Fig. 6a, b). $rETR_{max}$ reflects the maximum photosynthetic capacity. The change of $rETR_{max}$ is attributed to the change of the capacity of the electron transport chain or Calvin cycle enzymes [47]. In the present study, the RLCs of $rETR_{max}$(II) significantly dropped under Cu^{2+} stress, implying that the adaptability of electron transport in PSII is significantly reduced. Similarly, Zhou et al. [43] reported that $rETR_{max}$ of PSII of *M. aeruginosa* significantly decreased under 2.5 μM $CuSO_4$. Cu^{2+} (100 $\mu g\ L^{-1}$) had slight inhibition of the RLCs of $rETR_{max}$(I), which led to the slight decline of the RLC. The light adaptability of PSII was lower than that of PSI for all treatments, which is in agreement with some earlier studies [44]. I_k(II) of $rETR_{max}$(II) and I_k(I) of $rETR_{max}$(I) were increased at 10–50 $\mu g\ L^{-1}$ Cu^{2+} compared to control, indicating that low concentrations of Cu^{2+} increased the high light

adaptability of *M. aeruginosa*. When Cu^{2+} concentration was increased to 100 μg L^{-1}, Cu^{2+} toxicity triggered the photoinhibition of both PSI and PSII at light intensities lower than unstressed condition. Similar results were also observed for plants exposed to other heavy metals [16, 34, 46]. The similar response pattern of $rETR_{max}$(II) and $rETR_{max}$(I) to I_k(II) and I_k(I) indicates that low concentration of Cu^{2+} slightly stimulates the maximal electron transport rate in both PSI and PSII, but high concentration of Cu^{2+} reduced the maximal electron transport rate. α of RLC of $rETR_{max}$(I) or $rETR_{max}$(II) reflects the quantum yield of PSI or PSII [33]. The present study showed that α(II) in $rETR_{max}$(II) decreased but α(I) in $rETR_{max}$(I) increased after exposure to Cu^{2+}, which was in accordance with the changes of quantum yield of PSII [*Y*(II)] and PSI [*Y*(I)].

CEF around PSI is essential for preventing damage by dissipating excess photon energy [48]. CEF has been found to be stimulated under some stressful conditions [49]. In the present study, *Y*(CEF) under Cu^{2+} stress increased significantly (Fig. 4a). The increase of CEF implies the stimulation of the protection mechanism for PSI [50] and PSII. In other words, CEF can transfer electrons from PSI to PQ and protect PSII through dissipation of excess energy and prevent acceptor side limitation of PSI [48, 50]. Ouzounidou et al. [51] also found that PSI was less inhibited under Cu^{2+} stress, accompanied with an increase of cyclic electron transport. It is generally held that PSI electron transport is less sensitive to many environmental stresses than PSII [13]. *Y*(CEF) was negatively correlated with F_v/F_m in the present study (Fig. 5), suggesting that the stimulation of CEF is positively correlated with the extent of PSII photodamage, which was in consistent with the report by Huang et al. [30]. Under environmental stress, the stimulated CEF contributes to the buildup of a trans-thylakoid membrane proton gradient which induces more synthesis of ATP. More synthesized ATP could be used for the repair of photodamaged PSII subunits [30, 52].

The increases of *Y*(CEF)/*Y*(I) and *Y*(CEF)/*Y*(II) with increasing Cu^{2+} concentration (Fig. 4b) indicate the contribution of CEF to counteracting the inhibitory effect of Cu^{2+} on PSII and PSI. On the contrary, *Y*(II)/*Y*(I) decreased with increasing Cu^{2+} concentration, which indicates the decrease of the contribution of LEF to *Y*(I). Inhibition of LEF from PSII to PSI could be useful for alleviating the damage to PSI [53] and keeping the stability of PSI. The decrease of the ratio of *Y*(II)/*Y*(I) with increasing Cu^{2+} concentration showed the imbalanced distribution of quantum yield between PSII and PSI with more inhibition of PSII than PSI.

In conclusion, Cu^{2+} treatment had significant inhibitory effects on cell growth and Chl *a* synthesis of *M. aeruginosa*. The activities and electron transport rate of PSII was significantly suppressed by excess Cu^{2+}, while PSI quantum yield was slightly increased due to activation of cyclic electron flow around PSI. The stimulating effect of excess Cu^{2+} on PSI activity needs further study.

Acknowledgments This work was supported by the the National Natural Science Foundation of China (U1120302 and 21177127) and the Specialized Research Fund for the Doctoral Program of Higher Education (20125303120003).

Conflict of interest The authors declare that there are no conflicts of interest.

References

1. Küpper H, Šetlík I, Spiller M, Küpper FC, Prášil O (2002) Heavy metal-induced inhibition of photosynthesis: targets of in vivo heavy metal chlorophyll formation. J Phycol 38:429–441
2. Roussel H, Ten-Hage L, Joachim S, Cohu RL, Gauthier L, Bonzom J-M (2007) A long-term copper exposure on freshwater ecosystem using lotic mesocosms: primary producer community responses. Aquat Toxicol 81:168–182
3. Elder JF, Horne AJ (1978) Copper cycles and $CuSO_4$ algicidal capacity in two California lakes. Environ Manag 2:17–30
4. Nikookar K, Moradshahi A, Hosseini L (2005) Physiological responses of *Dunaliella salina* and *Dunaliella tertiolecta* to copper toxicity. Biomol Eng 22:141–146
5. Qian HF, Li JJ, Sun LW, Chen W, Sheng GD, Liu WP, Fu ZW (2009) Combined effect of copper and cadmium on *Chlorella vulgaris* growth and photosynthesis-related gene transcription. Aquat Toxicol 94:56–61
6. Qian HF, Yu SQ, Sun ZQ, Xie XC, Liu WP, Fu ZW (2010) Effects of copper sulfate, hydrogen peroxide and N-phenyl-2-naphthylamine on oxidative stress and the expression of genes involved photosynthesis and microcystin disposition in *Microcystis aeruginosa*. Aquat Toxicol 99:405–412
7. Backor M, Záczi P (2002) Copper tolerance in the lichen photobiont *Trebouxia erici* (Chlorophyta). Environ Exp Bot 48:11–20
8. Oukarroum A, Perreault F, Popovic R (2012) Interactive effects of temperature and copper on photosystem II photochemistry in *Chlorella vulgaris*. J Photochem Photobiol B Biol 110:9–14
9. Küpper H, Küpper F, Spiller M (1996) Environmental relevance of heavy metal-substituted chlorophylls using the example of water plants. J Exp Bot 47:259–266
10. Cid A, Herrero C, Torres E, Abalde J (1995) Copper toxicity on the marine microalga *Phaeodactylum tricornutum*: effects on photosynthesis and related parameters. Aquat Toxicol 31: 165–174
11. Mijovilovich A, Leitenmaier B, Meyer-Klaucke W, Kroneck PMH, Götz B, Küpper H (2009) Complexation and toxicity of copper in higher plants. II. Different mechanisms for copper versus cadmium detoxification in the copper-sensitive cadmium/zinc hyperaccumulator *Thlaspi caerulescens* (Ganges Ecotype). Plant Physiol 151:715–731
12. Mishra S, Dubey RS (2005) Heavy metal toxicity induced alterations in photosynthetic metabolism in plants. In: Pressarakli M (ed) Handbook of photosynthesis. Taylor and Francis Group, CRC Press, Boca Raton, pp 845–863
13. Boucher N, Carpentier R (1999) Hg^{2+}, Cu^{2+}, and Pb^{2+}-induced changes in photosystem II photochemical yield and energy storage in isolated thylakoid membranes: a study using simultaneous fluorescence and photoacoustic measurements. Photosynth Res 59:167–174
14. Wu X, Hong FS, Liu C, Su MY, Zheng L, Gao FQ, Yang F (2008) Effects of Pb^{2+} on energy distribution and photochemical activity of spinach chloroplast. Spectrochim Acta A 69:738–742

15. Singh R, Dubey G, Singh VP, Srivastava PK, Kumar S, Prasad SM (2012) High light intensity augments mercury toxicity in cyanobacterium *Nostoc muscorum*. Biol. Trace Elem Res 149:262–272
16. Deng CN, Zhang DY, Pan XL, Chang FQ, Wang SZ (2013) Toxic effect of mercury on PSI and PSII activites, membrane potential and transthylakoid proton gradient in *Microsorium pteropus*. J Photochem Photobiol B Biol 127:1–7
17. Ouzounidou G (1996) The use of photoacoustic spectroscopy in assessing leaf photosynthesis under copper stress: correlation of energy storage to photosystem II fluorescence parameters and redox change of P700. Plant Sci 113:229–237
18. Yan K, Chen P, Shao H, Shao C, Zhao S et al (2013) Dissection of photosynthetic electron transport process in sweet sorghum under heat stress. PLoS ONE 8(5):e62100. doi:10.1371/journal.pone.0062100
19. Chen W, Yao X, Cai K, Chen J (2011) Silicon alleviates drought stress of rice plants by improving plant water status, photosynthesis and mineral nutrient absorption. Biol Trace Elem Res 142:67–76
20. Perreault F, Ali NA, Saison C, Popovic R, Juneau P (2009) Dichromate effect on energy dissipation of photosystem II and photosystem I in *Chlamydomonas reinhardtii*. J Photochem Photobiol B Biol 96:24–29
21. Coopman RE, Fuentes-Neira FP, Briceño VF, Cabrera HM, Corcuera LJ, Bravo LA (2010) Light energy partitioning in photosystems I and II during development of *Nothofagus nitida* growing under different light environments in the Chilean evergreen temperate rain forest. Trees 24:247–259
22. Leunert F, Grossart HP, Gerhardt V, Eckert W (2013) Toxicant induced changes on delayed fluorescence decay kinetics of Cyanoobacteria and green algae: a rapid and sensitive biotest. PLoS ONE 8(4):e63127. doi:10.1371/journal.pone.0063127
23. Stanier RY, Kunisawa R, Mandel M, Cohen-Bazire G (1971) Purification and properties of unicellular blue-green algae (*oder Chroococcales*). Bacteriol Rev 35:171–205
24. Pfündel E, Klughammer C, Schreiber U (2008) Monitoring the effects of reduced PS II antenna size on quantum yields of photosystems I and II using the Dual-PAM-100 measuring system. PAM Appl Notes 1:21–24
25. Hout Y, Babin M (2010) Overview of fluorescence protocols: theory, basic concepts and practice. In: Suggett DJ, Prášil O, Borowitzka MA, Prasil O (eds) Chlorophyll *a* fluorescence in aquatic sciences: methods and applications. Springer, London, p 59
26. Klughammer C, Schreiber U (2008) Complementary PS II quantum yields calculated from simple fluorescence parameters measured by PAM fluorometry and the Saturation Pulse method. PAM Appl Notes 1:27–35
27. Wang SZ, Chen FL, Mu SY, Zhang DY, Pan XL, Lee DJ (2013) Simultaneous analysis of photosystem response of *Microcystis aeruginoga* under chromium stress. Ecotoxicol Environ Saf 88: 163–168
28. Kramer DM, Johnson G, Kiirats O, Edwards GE (2004) New fluorescence parameters for the determination of Q_A redox state and excitation energy fluxes. Photosynth Res 79:209–218
29. Miyake C, Horiguchi S, Makino A, Shinzaki Y, Yamamoto H, Tomizawa K (2005) Effects of light intensity on cyclic electron flow around PSI and its relationship to non-photochemical quenching of Chl fluorescence in tobacco leaves. Plant Cell Physiol 46:1819–1830
30. Huang W, Zhang SB, Cao KF (2010) Stimulation of cyclic electron flow during recovery after chilling-induced photoinhibition of PSII. Plant Cell Physiol 51:1922–1928
31. Schreiber U, Klughammer C (2012) Assessment of wavelength-dependent parameters of photosynthetic electron transport with a new type of multi-color PAM chlorophyll fluorometer. Photosynth Res 113:127–144
32. Platt T, Gallegos CL, Harrison WG (1980) Photoinhibition of photosynthesis in natural assemblages of marine phytoplankton. J Mar Res 38:687–701
33. Saroussi S, Beer S (2007) Alpha and quantum yield of aquatic plants derived from PAM fluorometry: uses and misuses. Aquat Bot 86:89–92
34. White S, Anandraj A, Bux F (2011) PAM fluorometry as a tool to assess microalgal nutrient stress and monitor cellular neutral lipids. Bioresour Technol 102:1675–1682
35. Lichtenthaler HK, Wellburn AR (1983) Determination of total carotenoids and chlorophyll *a* and *b* of leaf extracts in different solvents. Biochem Soc Trans 603:591–592
36. Ling QF, Hong FS (2009) Effects of Pb^{2+} on the structure and function of photosystem II of *Spirodela polyrrhiza*. Biol Trace Elem Res 129:251–260
37. Suzuki K, Ohmori Y, Ratel E (2011) High root temperature blocks both linear and cyclic electron transport in the dark during chilling of the leaves of rice seedlings. Plant Cell Physiol 52:1697–1707
38. Papageorgio GC, Govindjee (2004) Chlorophyll a fluorescence: a signature of photosynthesis. Advances in photosynthesis and Respiration, vol 19. Springer, Dordrecht
39. Karukstis KK (1991) Chlorophyll fluorescence as a physiological probe of the photosynthetic apparatus. In: Scheer H (ed) Chlorophyll. CRC Press, London, pp 770–797
40. Ibelings BW, Kroon BMA, Mur LR (1994) Acclimation of photosystem-II in a cyanobacterium and a eukaryotic green-alga to high and fluctuating photosynthetic photon flux densities, simulating light regimes induced by mixing in lakes. New Phyto 128:407–424
41. Campbell D, Hurry V, Clarke AK, Gustafsson P, Őquist G (1998) Chlorophyll fluorescence analysis of cyanobacterial photosynthesis and acclimation. Microbiol Mol Biol Rev 62:667–683
42. Toncheva-Panova T, Merakchiyska M, Djinggova R, Ivanova J, Sholeva M (2006) Effect of Cu^{2+} on the red microalga *Rhodella reticulata*. Gen Appl Plant Physiology (Special Issue) 53-60
43. Zhou S, Shao Y, Gao N, Deng Y, Qiao J, Ou H, Deng J (2013) Effects of different algaecides on the photosynthetic capacity, cell integrity and microcystin-LR release of *Microcystis aeruginosa*. Sci Total Environ 463–464:111–119
44. Wang SZ, Zhang DY, Pan XL (2013) Effects of cadmium on the activities of photosystems of *Chlorella pyrenoidosa* and the protective role of cyclic electron flow. Chemosphere 93:230–237
45. Dhir B, Sharmila P, Saradhi PP, Sharma S, Kumar R, Mehta D (2011) Heavy metal induced physiological alterations in *Salvinia natans*. Ecotoxicol Environ Saf 74:1678–1684
46. Wodala B, Eitel G, Gyula TN, Ődög A, Horváth F (2012) Monitoring moderate Cu and Cd toxicity by chlorophyll fluorescence and P_{700} absorbance in pea leaves. Photosynthetica 50:380–386
47. Ralph PJ, Gademann R (2005) Rapid light curves: a powerful tool to assess photosynthetic activity. Aquat Bot 82:222–237
48. Munekage Y, Mihoko H, Miyake C, Tomizawa KI, Endo T, Tasaka M, Shikanai T (2004) Cyclic electron flow around photosystem I is essential for photosynthesis. Nature 429:579–582
49. Gao S, Wang G (2012) The enhancement of cyclic electron flow around photosystem I improves the recovery of severely desiccated *Porphyra yezoensis* (Bangiales, Rhodophyta). J Exp Bot 63:4349–4358
50. Takahashi S, Milward SE, Fan DY, Chow WS, Badger MR (2009) How does cyclic electron flow alleviate photoinhibition in *Arabidopsis*? Plant Physiol 149:1560–1567
51. Ouzounidou G, Lannoye R, Karataglis S (1993) Photoacoustic measurements of photosynthetic activities in intact leaves under copper stress. Plant Sci 89:221–226
52. Allakhverdiev SI, Nishiyama Y, Takahashi S, Miyairi S, Suzuki I, Murata N (2005) Systematic analysis of the relation of electron transport and ATP synthesis to the photodamage and repair of photosystem II in *Synechocystis*. Plant Physiol 137:263–273
53. Kudoh H, Sonoike K (2002) Irreversible damage to photosystem I by chilling in the light: cause of the degradation of chlorophyll after returning to normal growth temperature. Planta 215:541–548